Materiales de Construcción 75 (360)
October-December 2025, e391
ISSN-L: 0465-2746, eISSN: 1988-3226
https://doi.org/10.3989/mc.2025.396424

Directional-sequenced magnetic pulses: a novel method to improve the alignment index of steel fibers through homogeneous magnetic fields in cementitious composites

N. Flores Medina[a]✉, L. Trigo Ramírez[a], V. Pérez Villar[a], V.M. Cabrera García[a], F. Gil Carrillo[b]

a. Departamento de Construcción Arquitectónica, Campus Universitario de Tafira s/n, Las Palmas de Gran Canaria, (Gran Canaria, Spain)
b. Departamento de Construcciones Arquitectónicas y su control, Escuela Técnica Superior de Edificación, Universidad Politécnica de Madrid, (Madrid, Spain)
✉: Nelson.flores@ulpgc.es

Received 15 October 2024
Accepted 06 April 2025
Available on line dd month year 09 January 2026

ABSTRACT: Directional-sequenced magnetic pulses (D-SMP) are a method to achieve a better alignment index of reinforcing steel fibers in Concrete with the same device at the same magnetic field. The optimal angles to apply the magnetic field are obtained through the analysis of the angular rotation of the fibers for a determined magnetic field and the Yield Stress (T_0) of the matrix. The method has been studied for three commercial Hooked-end-fibers (HSFs) commonly used as reinforcement in cementitious composites in a transparent fluid with a similar T_0 to that of cement composites. The efficiency of the D-SMP method is determined through directional statistics, setting the alignment index and the mechanical efficiency factor of the composite. The results obtained demonstrate that the D-SMP method results in a higher angular homogeneity of fibers, alignment index and efficiency factor than the use of a magnetic field in a single direction.

KEY WORDS: Steel fiber alignment; Cementitious composites; Mechanical fiber efficiency; Directional statistics.

Citation/Citar como: Flores Medina N, Trigo Ramírez L, Pérez Villar V, Cabrera García VM, Gil Carrillo F. 2025. Directional-sequenced magnetic pulses: a novel method to improve the alignment index of steel fibers through homogeneous magnetic fields in cementitious composites. Mater. Construcc. 75(360):e391. https://doi.org/10.3989/mc.2025.396424

RESUMEN: *Pulsos magnéticos en secuencias direccionales: un nuevo método para mejorar el índice de alineación de fibras de acero a través de campos magnéticos homogéneos en materiales compuestos de base cementicia.* Los pulsos magnéticos en secuencias direccionales como método consiguen un mejor índice de alineación de las fibras de acero de refuerzo en hormigón empleando el mismo dispositivo y campo magnético. Los ángulos óptimos para aplicar el campo magnético se obtienen mediante el análisis de la rotación angular de las fibras para un campo magnético determinado y la tensión de fluencia (T0) de la matriz. El método se ha estudiado para tres fibras comerciales, comúnmente utilizadas como refuerzo en compuestos cementicios, en un fluido transparente con una T0 similar a otros materiales cementicios. La eficiencia del método se determina mediante estadísticas direccionales, estableciendo el índice de alineación y el factor de eficiencia mecánica del material compuesto. Los resultados obtenidos muestran una mejora en la homogeneidad angular de las fibras, en el índice de alineación y en el factor de eficiencia que el uso de un campo magnético en una sola dirección.

PALABRAS CLAVE: Alineamiento de fibras de acero; Compuestos cementosos; Eficiencia mecánica de las fibras; Estadísticas direccionales.

1. INTRODUCTION

Fibers are used as a reinforcement in cementitious composites, improving their mechanical properties, reducing cracking during setting or during lifetime, and increasing their durability, etc. (1). Matrices and fibers may be produced from different materials and processes of origin, and they will be selected depending on their final use or cost. For a Fiber Reinforced Cementitious Composite (FRCC), one of its main problems is the rheology of its matrix as it settles during manufacture. Moreover, the fibers shape factor and flexibility must be studied as they modify the rheological properties of the composite and may also limit their volume fraction as fibers increase the shear stress of the fresh sample (2). When fibers must be aligned in a composite, more effort is needed to understand the rheology of the matrix alone and of the matrix reinforced with fibers (3).

Methods to align fibers during casting, pumping, or pouring into a mold have been studied deeply in the literature. In these cases, the rheology of the mixture with fibers must be studied and effects such as wall effects and the regime of the flow must be estimated. On the other hand, for magnetic fibers, alignment mainly depends on the rheological properties of the matrix as it is applied after the composite is cast. This can be considered as fibers are not dependent on the position of other fibers unless a high Volume Fraction (VF) of fibers are used and may interact (3).

It is important to note that some matrices may present rheological properties which also may vary during casting, increasing the opposition to fiber orientation. Moreover, some matrices may present Static Yield Stress (T_0^s), behaving as a Bingham, Herschel-Bulkley fluids or bilinear depending on the shear rate, and may also present thixotropic behavior (4). The relationship between rheology and manufacturing time must be set previously for the manufacture of any composite. To rotate, the fiber must exceed the momentum related to the T_0^s of the matrix and during rotation to the viscosity (S) of the sample (shear stress/shear rate).

The magnetic alignment of fibers, as reinforcement in cementitious composites, has been studied in cementitious matrices attending to their mechanical improvement, such as fiber reinforced concrete (5-8), self-compacting concrete (9), and Ultra High Performance Concrete (10), or attending to their flow behavior (11). The magnetic devices may use ranged simple coils, to a more complicated distribution of pair of coils (Helmholtz coils), but also some studies use ferromagnetic blocks. When Helmholtz coils are used a homogeneous magnetic field is presented mainly in the volume enclosed between coils which generates pure alignment without displacement. However, long periods of exposure to the magnetic fields on the sample may produce fiber entanglement losing the homogeneity and effectiveness of the composite (9). Long time of exposure also requires higher energy costs and the device coils can become overheated, requiring extra cooling systems (12). Moreover, long periods of exposure may also facilitate the rebuilding of the shear stress of the matrix (13), reducing the fiber rotation.

In a previous research work (14) the improvement of fiber alignment in a Bingham matrix was settled through short time, homogeneous magnetic pulses with different intensities in one direction (DMP). The importance of the initial angle between the fiber and the magnetic field, the shape factor and flexibility of fiber was observed. The optimum angles for fiber rotation were studied later, as small angles will present low magnetic momentum (Equation [1]) and those with angles near 90º will show high magnetic momentum but higher angular distance.

$$|\overrightarrow{\mathbf{m}}_f| = \ell S |\overrightarrow{\mathbf{B}}_n| \qquad [1]$$

Where $|m_f|$ is the magnetic moment, l is the length of the fiber (m), S is the fiber section (m^2), and $|B_n|$ is the perpendicular induction.

On the other hand, the magnetic saturation of the fiber also plays an important role and is higher when the fiber is parallel to the magnetic field. This also creates a behavior in the fibers when they rotate that varies from parallel to the orthogonal position but finds the lowest value at these positions.

$$|\overrightarrow{\tau}_M| = \ell S |\overrightarrow{\mathbf{H}}| \mathcal{H}_B(|\overrightarrow{\mathbf{H}}| \cos\theta) \sin\theta \qquad [2]$$

Where l is the length of the fiber (m), and S the section (m^2), and θ is the angle of the magnetic axis of the fiber with respect to the exciting homogeneous field H exerted by the Helmholtz coil. H_B is the characteristic hysteresis cycle of the ferromagnetic fiber material. This behavior is important since it can reduce or cancel the magnetic torque when the fiber is at 0º or at 90º to the magnetic field (15).

To align the fibers using magnetic fields within the matrix, the magnetic torque must overcome the rheological torque and the inertia of the fiber (Equation [3]). Hence, to align fibers in the composite several options can be taken into account to ease the process according to the literature:

- The rheological properties of the matrix should be less onerous, as the design of the matrix can be settled with low static yield stress T_0^s and low viscosity S when manufactured, but also kept in time if the manufacture process stalls. To attend to this, several studies are focused on the use of the method in ultra high performance concrete (16). Mixture design must present a low aggregate fraction, with maximum aggregate diameter under 4 mm, a high volume fraction of fillers and fine additions to keep high viscosity and avoid segregation and high dosage of plasticizer to reduce T_0 (17);
- Vibration of the matrix during the alignment process also reduces the T_0 from static (T_0^s) to a dynamic (T_0^d) usually several times lower (thixotropy of the matrix). But segregation may be observed and lower homogeneity in the section of the composite (18); and
- The magnetic device can be oversized, to generate a higher magnetic torque but this can also be expensive especially in high-size constructive elements, as the magnetic field is reduced as the ratio of the coil is increased.

$$\underbrace{\ell S|\vec{H}(t)|\mathcal{H}_B(|\vec{H}(t)|\cos\theta)\sin\theta}_{\text{MagneticTorque}} = \underbrace{Y_R(S_{fo}, T_o^{(d)}, T_o^{(e)}, \dot{\theta})}_{\text{RheologicalTorque}} + \underbrace{I\ddot{\theta}}_{\text{Inertia}} \quad [3]$$

However, the mass of the fiber to increase the magnetic response and its geometry (straight, hooked-end, twisted…) and its shape ratio (length and diameter ratio), as this affects the fiber hydrodynamics must be also considered as relevant (5, 18). Finally, the ferromagnetic properties of the steel's coercive and saturation field to define the magnetic hysteresis should be considered.

In this research work, the authors studied a method to increase the fiber alignment for a determined matrix without modifying its rheological properties and using the same magnetic field. For this, firstly, the angular response of Hooked-end Steel Fibers (HSF) exposed to a determined $|B_n|$ was studied in a matrix with a determined T_0^s similar to cementitious composites (explained later in Section 2). The results analyzed through directional statistics determined the angles in which the fiber dynamic is activated (aligning window) and those angles where the fibers cannot overcome the matrix rheology and do not rotate (dead zones- with no fiber response). When this optimal angle is obtained, the process consists of rotating the sample and generating a first magnetic pulse at the optimized angle and rotating the sample again to generate a second pulse at the opposite angle. This method based on sequenced-directional magnetic pulses (D-SMP) is compared in its effectiveness to the previous system (14) based on a direct magnetic pulse (DMP) to align the fibers. The alignment index and the mechanical efficiency factor (Cox-Krenchel model) are also studied for each HSF and each magnetic field. The results obtained demonstrate that the D-SMP method results in a better angular homogeneity of fibers as does the alignment index and the efficiency factor. These were also improved when the D-SMP method is used in comparison with the DMP method reducing the amount of HSF in misaligned angles with low mechanical contribution.

2. MATERIALS AND TEST METHODS

The method followed a continuation of procedures and materials already described in previous research work using a single-axis alignment method with Helmholtz coils (14).

2.1. Materials

The following materials have been studied to determine the alignment of fibers in matrices with T_0^s or also known in rheological terms as Bingham or Herschel-Burkley models, depending later on their behavior under a determined shear rate (19).

Matrix: a transparent matrix with Carbopol 940 was selected as a metaphor fluid, adjusting its static yield stress T_0 with a value of 20 Pa according to a concentration (0.2% w/w) and pH 7 measured on the sample (20). This T_0^s is similar to other matrices, such as cement paste, mortar or self-compacting concrete (21-22).

The hydrogel matrix was prepared at 25ºC in two stages (23). Firstly, the sample was hydrated by agitation with a magnetic stirrer at 600 rpm. Once the Carbopol is completely dissolved, the dispersion is left static for 30 minutes for full hydration and elimination of any air bubbles that may have been generated during stirring. Secondly, the pH neutralization is obtained by adding triethanolamine ($C_6H_{15}NO_3$) accompanied by a gentle agitation to avoid the formation of air bubbles. The dispersion stays at rest for 24h before testing.

Fibers: three fibers with the same steel composition but different lengths and shape factors were used. The fibers are hooked end, DRAMIX 3D series, manufactured by Bekaert™. Their geometric and physical properties are summarized in Table 1. The magnetic moment of the fibers was determined in previous work (14) and tested later by others (24).

Table 1. Physical properties of the fibers studied.

Type of fiber	l_f (mm)	d_f (mm)	l_f / d_f	m (g)	m/(l_f / d_f)	E (MPa)
45/50 BL	50	1,05	47,6	0,35	0,00740	210.000
65/60 BG	60	0,9	66,7	0,32	0,00480	210.000
80/60 BG	60	0,75	80	0,22	0,00275	210.000

2.2. Magnetic alignment device

Two coils following the Helmholtz geometry (14) were manufactured along the outside of a PVC plastic cylinder, diameter 160 mm with a coil of 16 AWG copper coated wire and diameter 1.5 mm. The value of magnetic field inside of the coil was determined using the Maxwell Equations (Ampere's law) (7). The coil winding was 100 turns, and the peak electric intensity (I_{Max}) generated during the discharge and the peak of the magnetic field (B_{Max}), together with the RMS (Root Mean Square) value B_{RMS} of such magnetic field peak generated by the Hemholtz coil are summarized in Table 2:

Table 2. Characteristics of the magnetic field obtained at different intensities.

V_0 (V)	I_{max} (A)	μ_0H (RMS)	B_{max} (mT)	B_{RMS} (mT)
100	21	30	43,33	20,61
140	29	69	60,65	28,85
180	37	78	77,98	37,09

2.3. Experimental outline

Two magnetic alignment methods have been compared, DMP and D-SMP. Firstly, the authors studied the possibility of improving fiber alignment through setting a sequence of DMP. However, the fibers after the first pulse did not show any improvement when the direction of the magnetic pulse was not modified. Hence D-SMP was proposed based on the study of the response/non response of the fibers. In the experimental campaign, three different types of fibers were exposed to three different magnetic field peaks. This sets a campaign of nine tests that would each be repeated seven times to compute a statistical average. In every test, ten fibers were used obtaining seventy responses for each one. Every set of ten fibers was randomly arranged and immersed in a volume of 500 ml of Carbopol 0.2% solution. This alignment process using several pulses for fibers for reinforcing the matrix in cementitious composites consisted of:

1. Firstly, setting the optimal angle is the studied according to the steel fiber characteristics, the magnetic field alignment and the rheological properties of the matrix. For this, a single magnetic pulse is performed for a batch of fibers in different orientations. In Figure 1 a sample of a mixture of a composite can be observed where the angle of each fiber has been determined before and after the magnetic pulse. From this study, the angles where the steel fibers do not rotate (dead zone) and the fiber response in the angles of the 'window' or range of angles where the fibers react (alignment window), are determined. The fiber response is the angular difference between the initial angle and the final angle of the fiber, after the alignment method is applied.
2. The sample is placed in the middle of the Helmholtz coil where a homogeneous field is generated. The sample is rotated manually to the angle Θ_2 firstly, and later $-\Theta_2$, Θ_2 is the limit where the fibers do not rotate as the magnetic torque cannot overcome the rheological properties of the matrix (especially the static yield stress; see Figure 2).
3. From observation, the Helmholtz coils do not really set the alignment direction directly as the sample is rotated. However, the fibers concentrate in the desired direction, to achieve the maximum rotation of the fibers increasing the alignment efficiency and the isotropy of the sample. Figure 3 represents the angles in which the fiber can be rotated and the angles in which the fibers will be more concentrated.

The desired angle of the first pulse can be also designed by setting the intensity of the field applied to each coil and at the same time to set a directional vector of the flux. As the equipment was not designed yet for this, the authors decided to set the angle by rotating the sample after the first pulse.

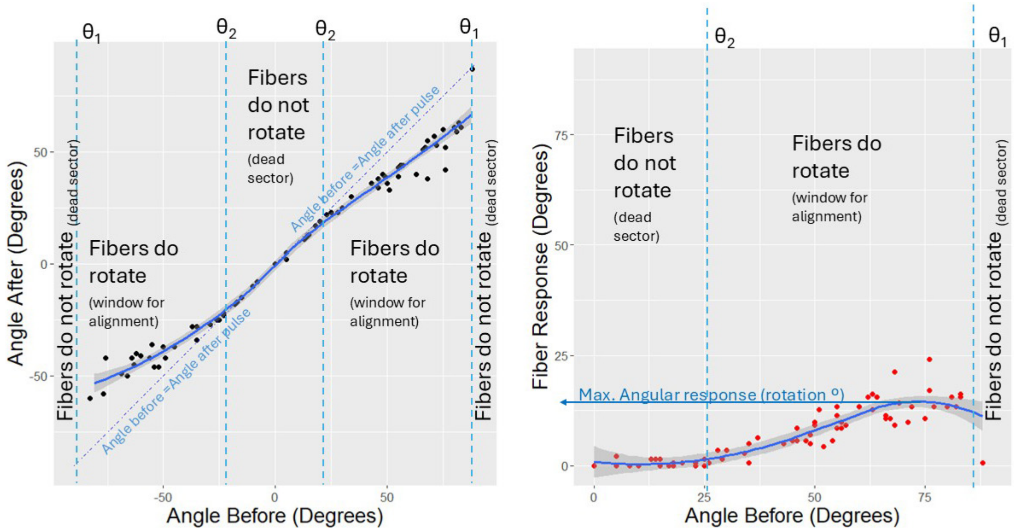

FIGURE 1. Preliminary study to determine the angles of the dead zones and the fiber response in the angles of the window or activation range.

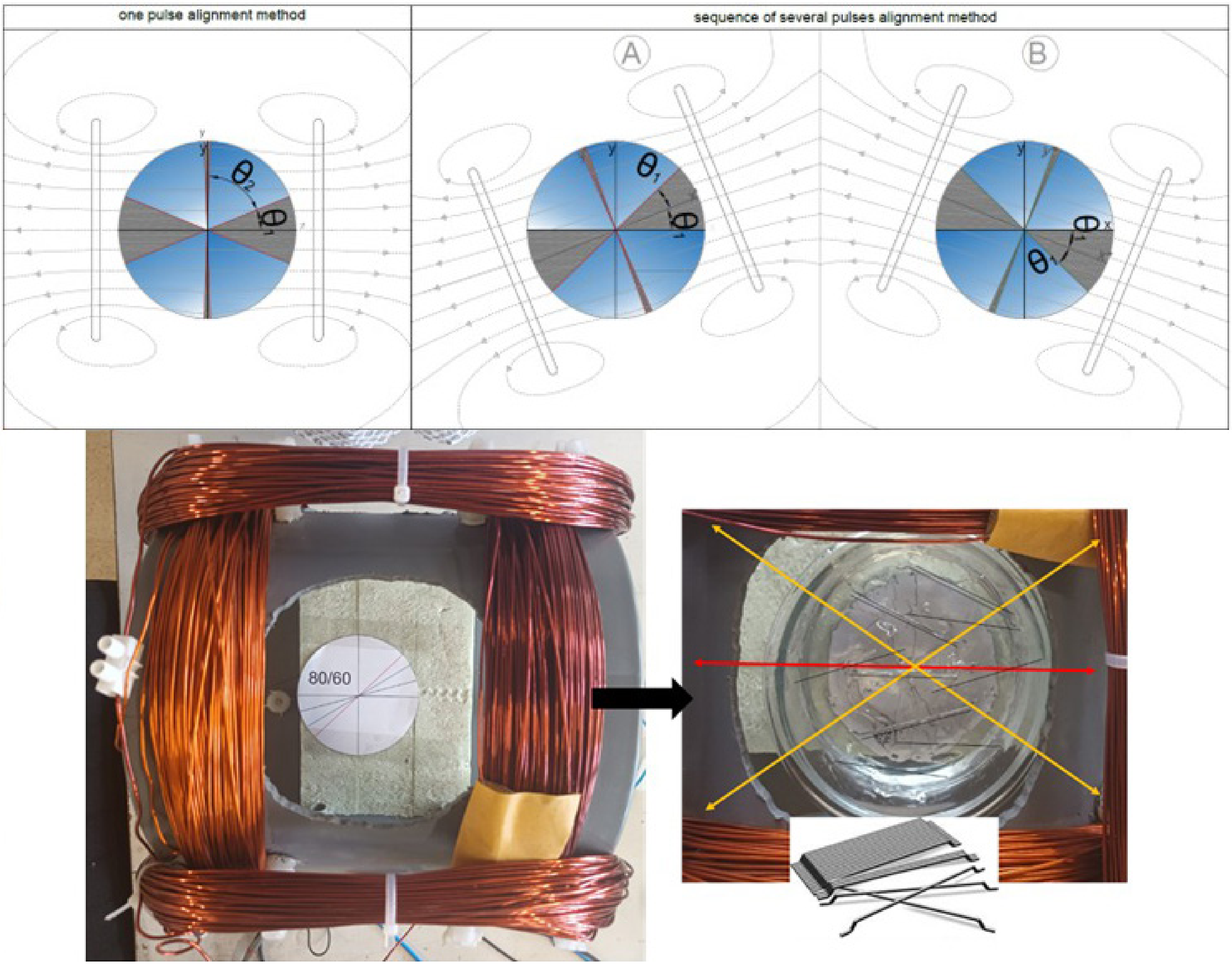

FIGURE 2. Angular rotation in the two pulse alignment process and the production setting with angular guides in the pair of coils before and after CAD treatment when $-\Theta_2$, Θ_2 are determined for each fiber and each field, H.

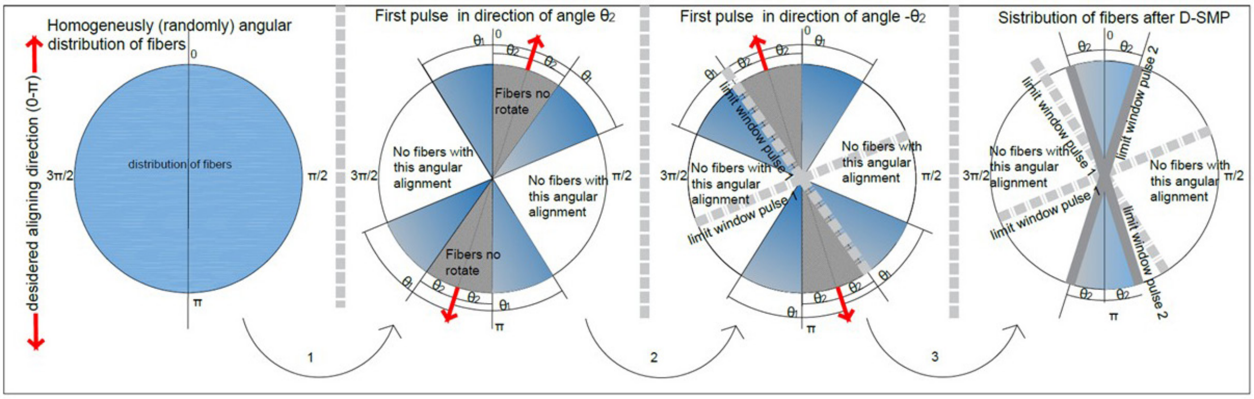

Figure 3. Alignment process through optimized directional pulses

2.4. Alignment index

Fiber alignment, in FRCC and other composites, is usually estimated through Equation [4] according to the specific literature. When η^{θ} is 0, fibers are badly aligned and present an orientation in the perpendicular direction to the one desired (isotropic 90º) and when is η^{θ} 1, the fibers are well aligned (isotropic 0º).

$$\eta^{\theta} = \frac{\sum_{0}^{i} cos\sigma}{n} \quad [4]$$

2.5. Fiber alignment through directional statistics. Median, quartiles and centroid

Fiber alignment can be studied using directional statistics to obtain more data about the angular distribution of the fiber in the composite (25-26). Directional data obtained through the measurement of the angles of the fiber in a matrix can be transformed into the directional data of a directional component of a dimensional vector, in our case in two dimensions. The directional statistics may be represented in circular means, from 0 to 180º reduced in this manuscript to analyze the alignment of fibers from 90º to -90º. This allows the geometrical interpretation of the fiber direction, obtaining not only the alignment but also the spread from a geometrical viewpoint (see Figures 4-11).

$$(\sin\theta i, \cos\theta i) \qquad i = 1,\dots,n \quad [5]$$

The Cartesian coordinates of the 'center of mass' ($\hat{R}$ can be obtained:

$$\hat{S} = \frac{1}{n}\sum_{i=0}^{n} sin\theta i \quad [6]$$

$$\hat{C} = \frac{1}{n}\sum_{i=0}^{n} cos\theta i \quad [7]$$

$\hat{C}$ is equal to the alignment index obtained in Equation 4. Hence, in directional study the alignment index is already included. The vector of the center of mass provides the fiber orientation and the length provides the spread of the batch studied, values near 0 indicate a high spread of the sample and the closer to 1 the nearest to the main angle and hence the angular homogeneity of the reinforcement of the composite:

$$\hat{R} = \vec{R} = \sqrt{\hat{S}^2 + \hat{C}^2} \quad [8]$$

$\vec{R}$, where the R value (centroid) is considered as the dispersion value of the circular data if R is zero the data is homogeneously dispersed and if R is 1 it is considered as concentrated near to the angular mean value, the circular mean orientation of fibers, which is obtained from the following expression:

$$\bar{\theta} = arctan\frac{\hat{S}}{\hat{C}} \qquad [9]$$

The angular distribution of fibers is studied in each step of the process. A batch of seven samples with ten fibers was randomly oriented and settled in the matrix manually avoiding any contact between fibers and modifications of the matrix rheology. The angular distribution was photographed first before the magnetic field was applied; then, after the first magnetic pulse; and finally, after the second magnetic pulse. The angle of the fibers in every step is analyzed through CAD (22). The difference between angles permits the following aspects of the angular distribution after DMP to be obtained, and of the angular distribution after D-SMP.

The angular distribution after each method was studied in circular statistics, setting the angles of median, quartiles and centroid. The width of the second and third of the quartiles helps to understand the distribution and concentration of the fibers in the desired direction and the homogeneity of the composite. The centroid sets the angular spread of fibers in the composite in the number of samples studied.

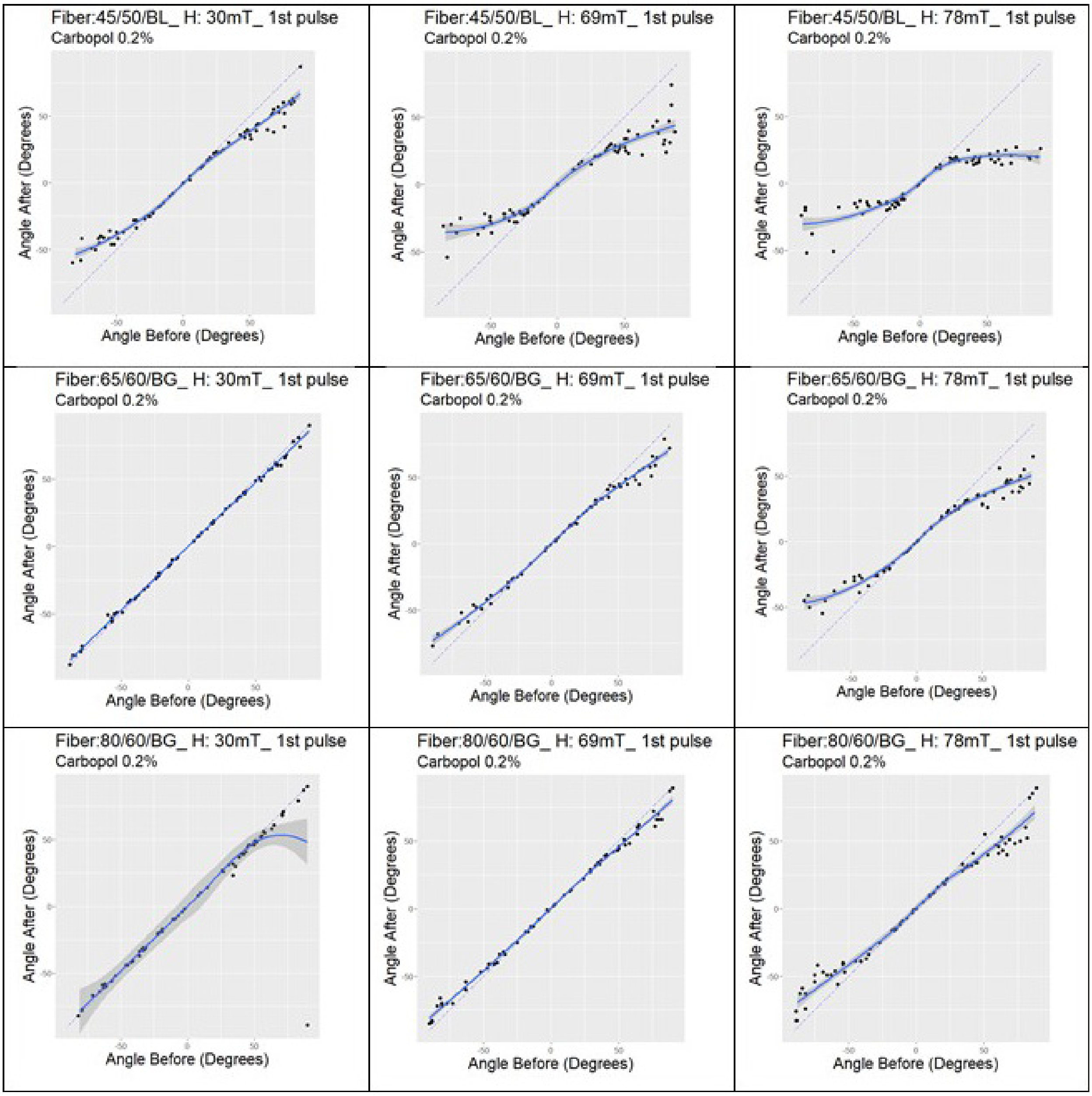

Figure 4. Initial angle vs. final angle after magnetic alignment through one pulse at different magnetic induction (30/69/78 mT) of 3 types of HSF.

2.6. Efficiency factor (aka Cox-Krenchel Efficiency)

To relate the fiber alignment and the composite mechanical characteristics, the efficiency factor ($\eta\theta_0$) has been applied following the Krenchel and Cox model (27-28). To integrate this theory with directional statistics, if we divide the circumference into k bins, the following expression can be proposed:

$$\eta_{\theta_o} = \sum_k \chi_k \cos^4\left(\theta_k - \theta_o\right) \qquad \text{Where} \qquad \eta_\theta \in [0,1] \qquad [10]$$

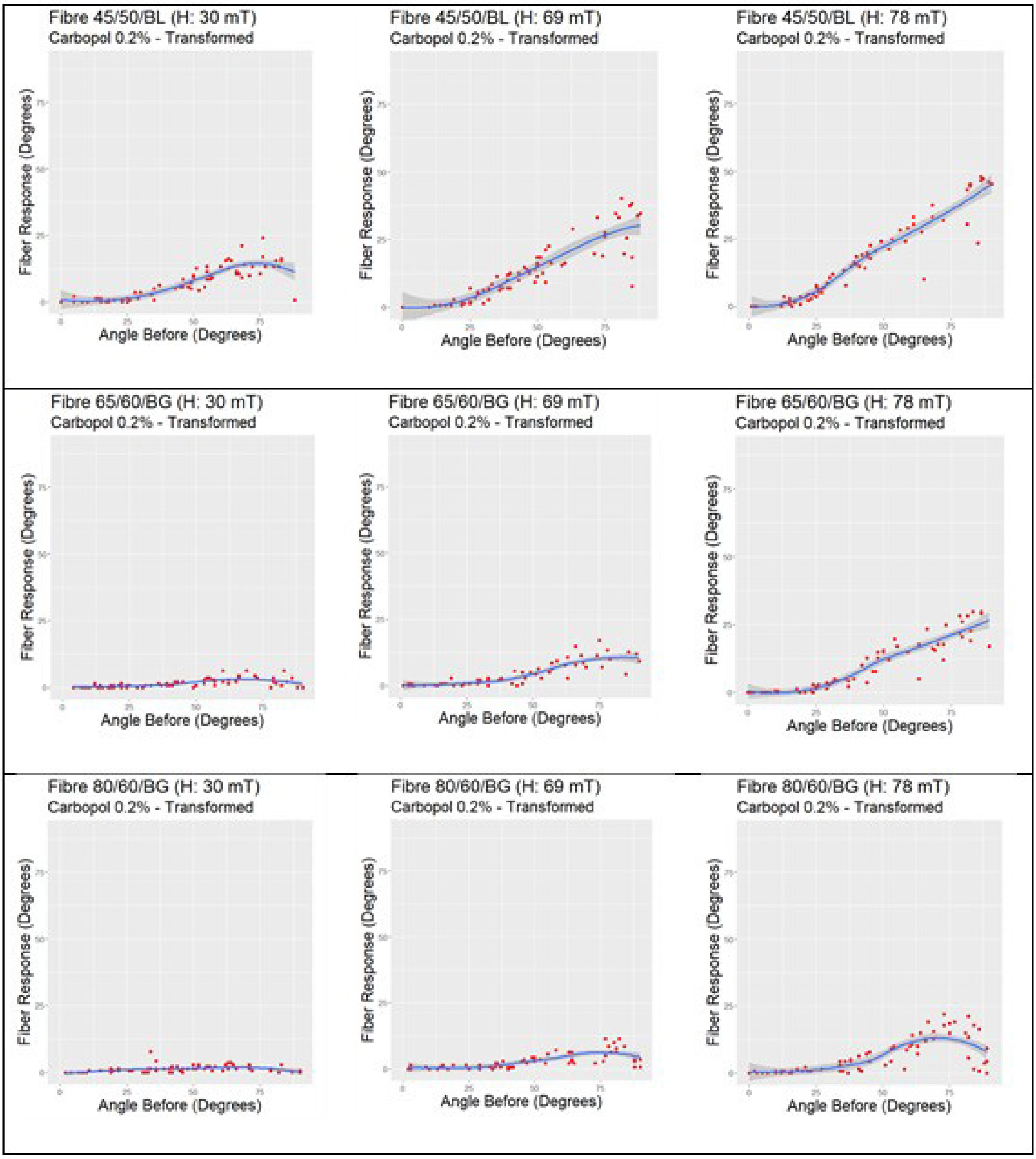

Figure 5. Initial angle vs. angular displacement after magnetic alignment through one pulse at different intensities (30/69/78 mT) of three types of fibers, previously magnetized and not magnetized.

Where X_k is the angular fraction of fibers content per bin and Θ_k is the representative fiber angle per bin with respect to the loading direction μo. We consider here Θ_0 is equal to zero, so we consider here the loading direction is coincident with the magnetic axes. If the Krenchel efficiency is equal to zero all the fibers are perpendicular to the coil axis, if η is equal to 0.375 it is considered random (homogeneous dispersed) and if η is equal to 1 all the fibers are aligned in the desired direction.

3. RESULTS AND ANALYSIS

The angles of rotation were recorded in each step before and after the magnetic alignment process was applied and (before; after one pulse; after two pulses; after four pulses) for each magnetic field pulse (30 mT ,69 mT, 78 mT) and for each fiber (45/50, 65/60, 80/60).

3.1. Determination of the range of rotation: window of activation and dead zone. Variation of orientation at one direct magnetic pulse (DMP) and angular displacement or fiber response

Figure 4 shows the results of angle of the fibers previously versus after the application of one pulse with the different magnetic fields. In this figure, the angles between 90 and – 90 can be observed where 0º is aligned. An auxiliary line at 45º has been plotted to represent those fibers with same angle before and after the magnetic field has been applied, meaning that they have not rotated. It can be observed that the higher the magnetic field, the lower the number of fibers following the line of no rotation. The angles between the fibers are different in every case, however Θ_2 is near 90º for every fiber as the magnetic torque drops drastically from the maximum value usually at 88º (Figure 4). On the other hand, Θ_1 varies more clearly for each fiber and magnetic pulse value. Fibers 45/50 present a Θ_2 almost constant of 88º and a Θ_1 of 18º for 30 mT, 8º for 69 mT and 5º for 78 mT. Fibers 65/60 show an activation window very narrow for 30 mT as the rotation is very slight from 87º Θ_2/55º Θ_1 but at 69 mT this presented a window from 85ºΘ_2 /33ºΘ_1 and 87ºΘ_2 /23º Θ_1 for a magnetic field equal to 79 mT. Results obtained for fiber 80/60, fibers did not show almost any reaction for 30 mT, but for 69 mT they showed a window from 83ºΘ_2 /48ºΘ_1, and for 78 mT from 85ºΘ_2 /35ºΘ_1.

The fibers response to the magnetic field is presented in Figure 5, comparing the angular rotation versus the angle before the magnetic alignment was exerted. In these charts, the angular displacement depending on the initial angle can be observed, which is higher in those close to the bisector drawn as a reference. Those initial angles with higher ascent are those with higher response. These charts help to understand the final position expected for each fiber and to set the fibers in the angles with higher rotation to achieve the best alignment success.

For fiber 45/50/BL when magnetic induction is 30 mT a maximum angular displacement of 25º was reached for fibers with initial angles between 75º/87º, 33º and 48º for fibers with initial angle of 87º at 69 mT and 78 mT respectively.

Fiber 65/60/BG presents a plateau response of 5º/7º for 69 mT when fibers are at an initial angle of 55/80º, but no response under or over this range. When the magnetic induction applied was 69 mT a maximum response of 15º can be observed at initial angles between 75º/87º and for 78 mT a maximum angular displacement of 27º for fibers with a previous angle of 87º.

The fiber response for 80/60/BG samples was almost null for 30 mT, and a very slight response of 12º for 69 mT and initial angle between 75/83º. When fibers were exposed to 78 mT the maximum fiber response was 23º for those fibers with initial angle from 75º to 80º.

3.2. Determination of fiber distribution and directional statistical analysis

In the following figures, fiber distribution of the fibers during the different alignment processes is studied through circular statistics. Firstly, the angular distribution of the batch of fibers randomly disposed in the matrix is always presented and before any magnetic field is applied. Secondly, the distribution of the fibers is presented after one direct directional pulse (DDP) in the alignment direction. The following charts on the right present the distribution of the fibers after D-SMP is applied, in two or four pulses, as each sequence needs two pulses at Θ_2 first and later -Θ_2 as explained in Section 3.1. In Table 3-4, statistical results detailing the angular fiber distribution are shown.

In Figure 6 the directional distribution of fiber 45/50 is presented before and after the magnetic pulse is applied at 30 mT , through DMP or D-SMP of two and four pulses. It can be observed that the angular concentration of the fibers is modified after each of the magnetic alignment methods studied are applied. In Table 3, after DMP the median has been set at 12.5º and the amplitude of fibers between second and third quartile is 72º with a centroid ($\bar{R}$) of 0.78. As the D-SMP of 2 pulses is applied to the composite, the median stays at 10.50º and the amplitude between second and third quartile is reduced to 56.25º and a centroid ($\bar{R}$) of 0.80. After four pulses of D-SMP are applied, the median is 21º, and the amplitude of the second and third quartile is again reduced to 45.25º and the centroid ($\bar{R}$) of 0.84.

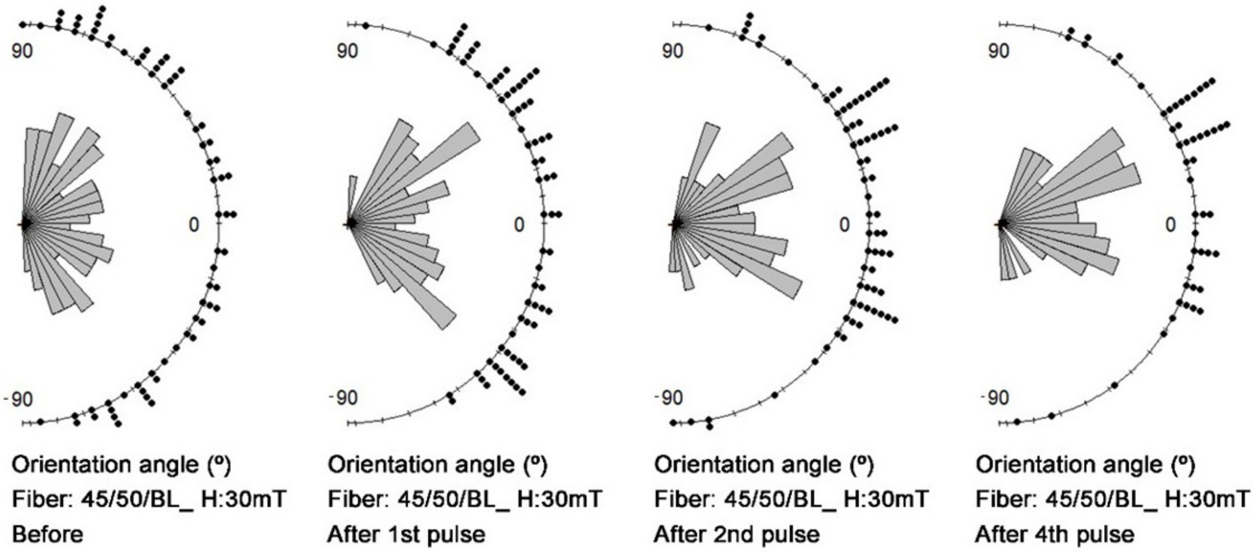

Figure 6. Directional distribution of fibers before and after magnetic alignment through DMP and D-SMP in 2 and 4 pulses of 30 mT at different planar angles of 45/50 fiber.

In Figure 7 the directional distribution of fiber 45/50 before and after the magnetic pulse is applied at 69 mT is presented graphically. The analysis of these charts is summarized in Table 3. It can be observed that after the application of DMP the median has been set at 11º and the amplitude of second and third quartile is 48.50º with a centroid ($\bar{R}$) of 0.88. As the D-SMP of 2 pulses is applied to the composite, the median stays in 10º and the amplitude between second and third quartile is reduced to 31.50º and a centroid ($\bar{R}$) of 0.92.

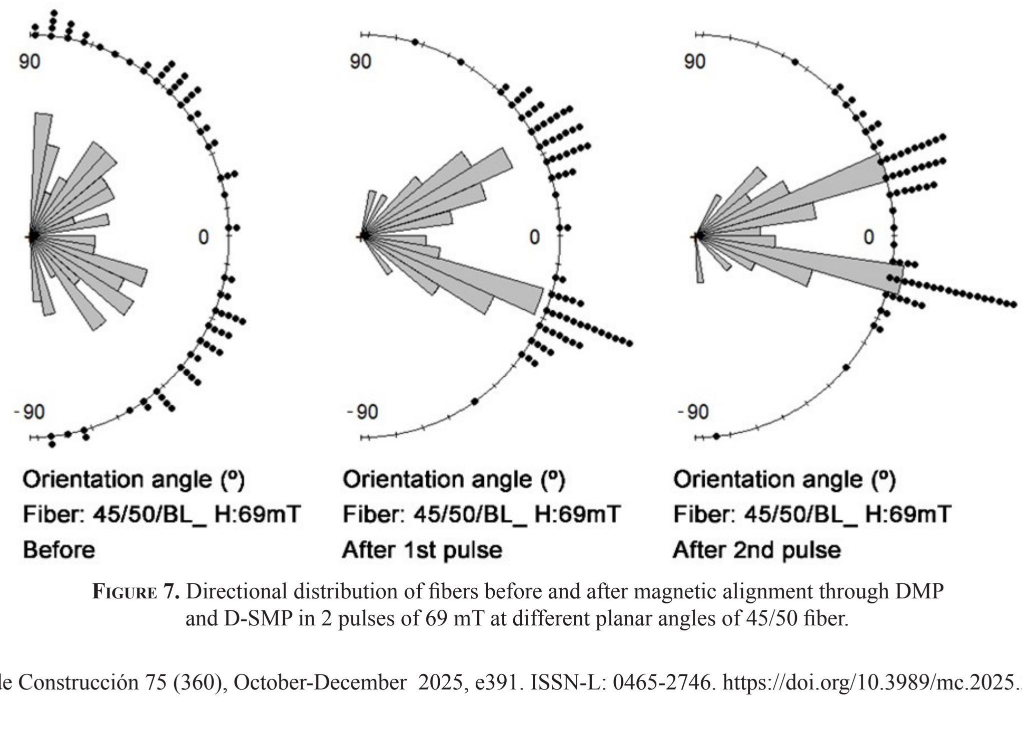

Figure 7. Directional distribution of fibers before and after magnetic alignment through DMP and D-SMP in 2 pulses of 69 mT at different planar angles of 45/50 fiber.

Figure 8 presents the directional distribution of fibers 45/50 before and after an H78 mT magnetic pulse was applied. From Table 3, it can be observed that after the application of DMP the median has been set at 11º and the amplitude of second and third quartile is 33º with a centroid ($\overline{R}$) of 0.95. After two pulses using the D-SMP method the median remains at 11º and but the amplitude of fibers between second and third quartile is concentrated at 25º and a centroid ($\overline{R}$) of 0.96.

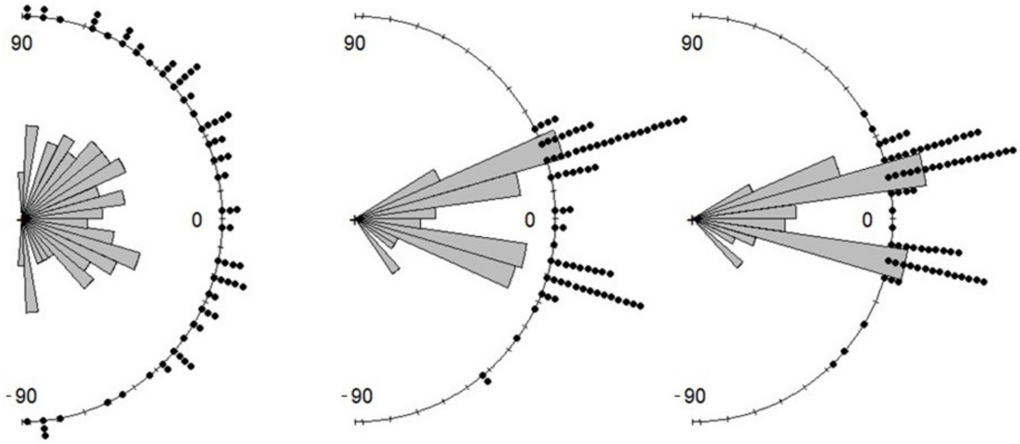

Figure 8. Directional distribution of fibers before and after magnetic alignment through DMP and D-SMP in 2 pulses of 78 mT at different planar angles of 45/50 fiber.

In Figures 9-11 the angular distribution of fibers 65/60/BG are drawn in charts of circular statistics. In the charts of Figure 6 the directional distribution of the fibers before and after H30 mT magnetic pulses are applied can be considered. From Table 4, it can be observed that after the application of DMP, the median has been set at 8º and the amplitude of second and third quartile is 75º with a centroid ($\overline{R}$) of 0.70. After two pulses using the D-SMP method the median is set at 4º and the amplitude of the second and third quartile is 75º and a centroid ($\overline{R}$) of 0.69. After the fourth pulse using the D-SMP method the median has settled at 5º, the amplitude of the second and third quartile at 74.25 and $\overline{R}$ of 0.68. The differences between samples in terms of fiber distribution after both alignment methods are applied are not significant.

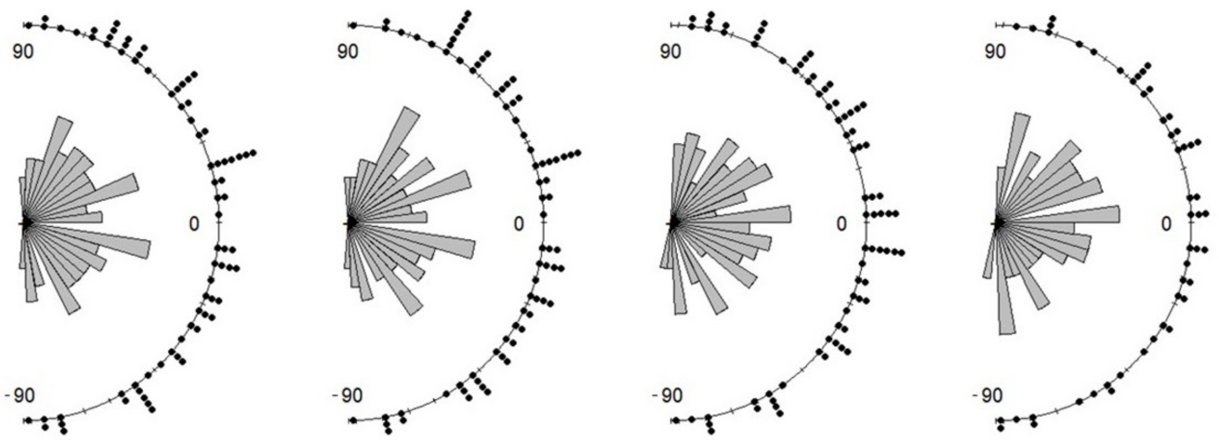

Figure 9. Directional distribution of fibers before and after magnetic alignment through DMP and D-SMP in 2 and 4 pulses of 30 mT at different planar angles of 65/60BG fiber.

Figure 10 presents the graphical angular distribution of the fibers before and after 69 mT magnetic pulses are applied. Detailed data has been summarized in Table 4, therefore it can be observed that after DMP the median of the distribution of fibers is 17º and the amplitude of second and third quartile is 69º with a centroid ($\bar{R}$) of 0.78. After two pulses using the D-SMP method the median is set at 23º and the amplitude of second and third quartile is 55º and $\bar{R}$ 0.80. After four D-SMPs the median is 20.50º, the amplitude of second and third quartile 56 and $\bar{R}$ 0.84.

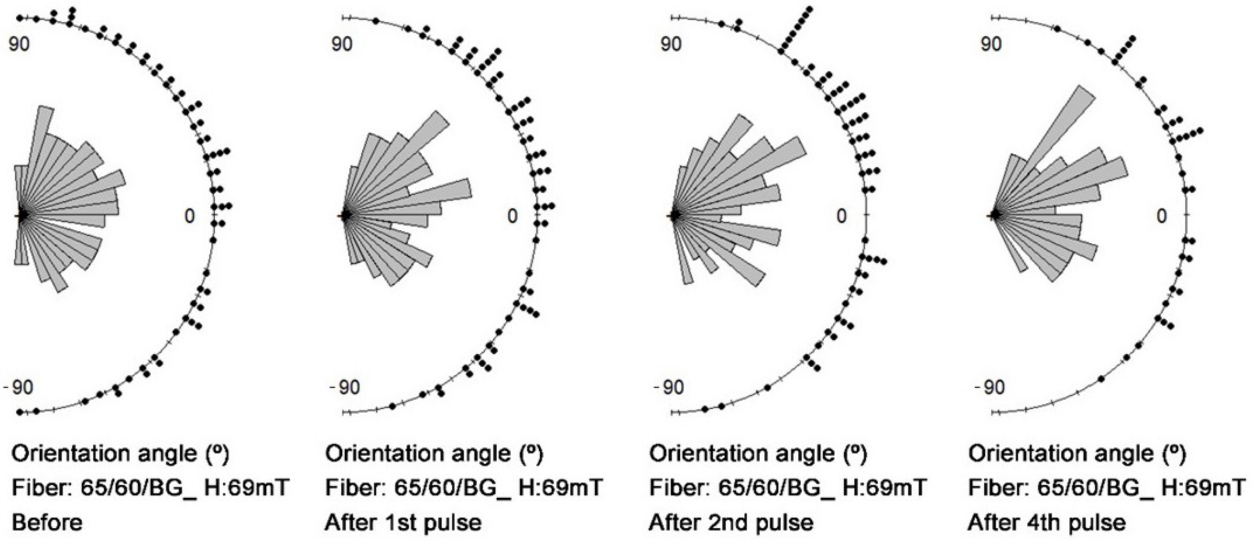

Figure 10. Directional distribution of fibers before and after magnetic alignment through DMP and D-SMP in 2 and 4 pulses of 69 mT at different planar angles of 65/60BG fiber.

Figure 11 shows the directional distribution of fibers 65/60/BG at H78 mT, before aligning and after the alignment through DMP or D-SMP of two and four pulses. After the DMP method is applied, the angular median is 14º and the amplitude of fibers between the second and third quartile is 56.5º, $\bar{R}$ of 0.85. As the D-SMP of two pulses is applied to the mixture, the median comes to 17.5º and the amplitude between the second and third quartile is reduced to 45.75º and a centroid ($\bar{R}$) of 0.90. After four D-SMPs the median comes to 5.5º, the amplitude of the second and third quartile is 41.25º and the centroid ($\bar{R}$) is 0.93.

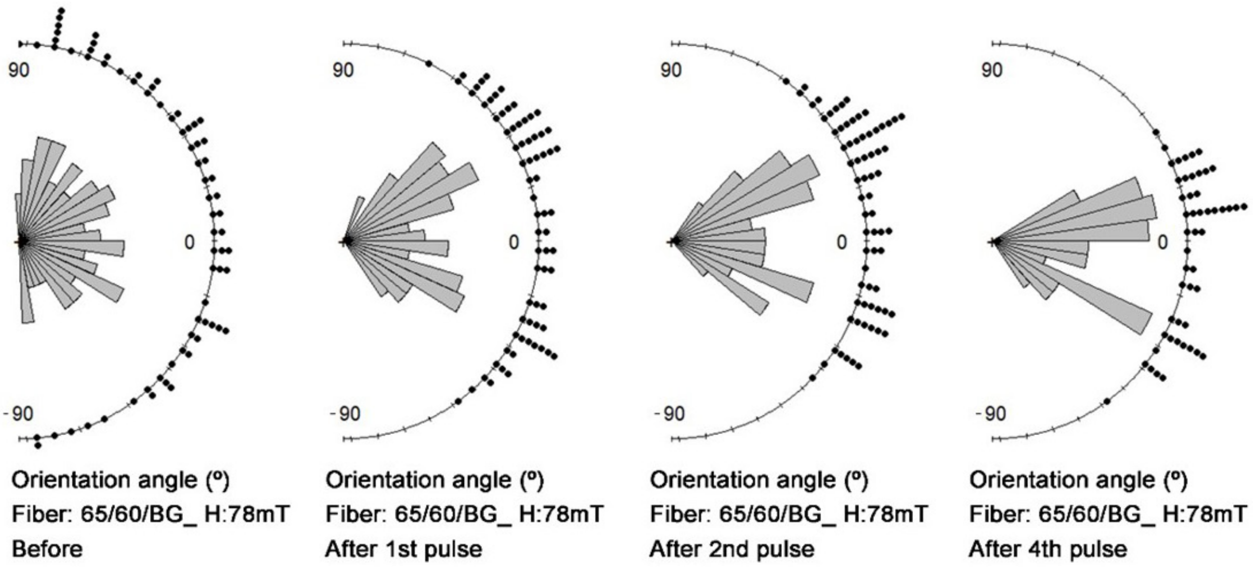

Figure 11. Directional distribution of fibers before and after magnetic alignment through DMP and D-SMP in 2 and 4 pulses of 78 mT at different planar angles of 65/60BG fiber.

In Figures 12-14 the angular distribution of fibers 80/60/BG after being exposed to magnetic fields of 30-69-78 mT are drawn in charts of circular statistics respectively. 80/60/BG fibers after DMP of H30 mT present a median of two with an amplitude of second and third quartiles of 81.5 and $\bar{R}$ of 0.69. When the magnetic field was also 30 mT, but using D-SMP the median was 4º, the amplitude 2º and 3º, quartile 83.5 and a $\bar{R}$ of 0.66, for two pulses and a median of 1º, amplitude of 2º and 3º, quartile of 83º and $\bar{R}$ of 0.65.

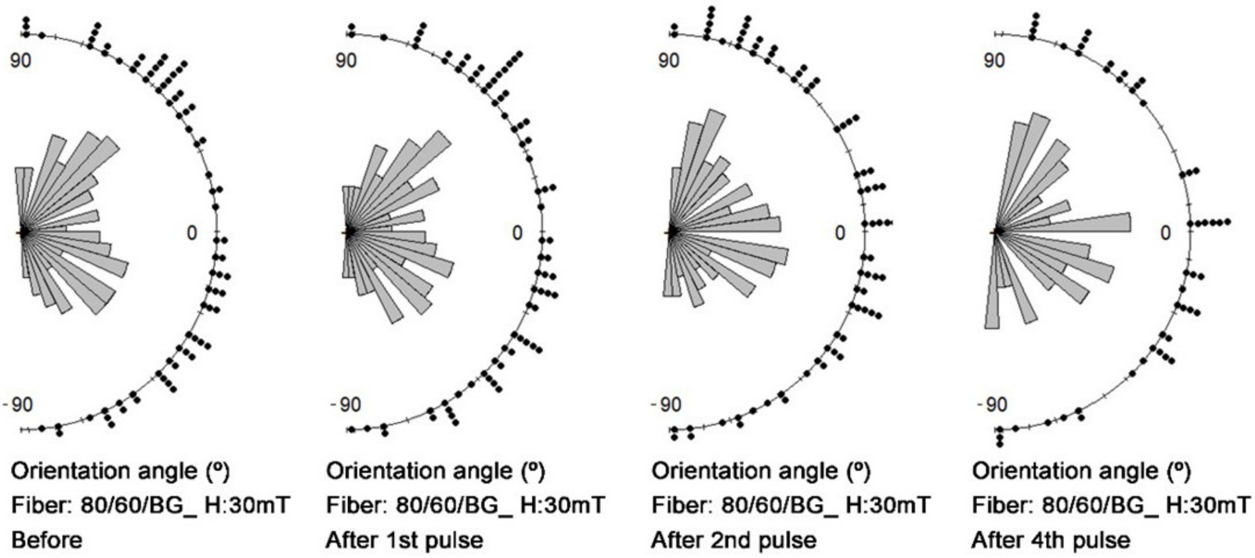

Figure 12. Directional distribution of fibers before and after magnetic alignment through DMP and D-SMP in 2 and 4 pulses of 30 mT at different planar angles of 80/60BG fiber.

Figure 13 shows the directional distribution of fiber 80/60/BG at 69 mT, before aligning and after the alignment through DMP or D-SMP of two and four pulses. After the DMP is generated, the angular median is 3º and the amplitude of second and third quartile is 85º, $\bar{R}$ of 0.67. As the D-SMP of two pulses is applied to the mixture, the median is 2º and the amplitude between second and third quartile 89º and a centroid ($\bar{R}$) of 0.68. After four D-SMPs the median shown is 11.5º, the amplitude of the second and third quartile is 70.75º and the centroid ($\bar{R}$) is 0.77.

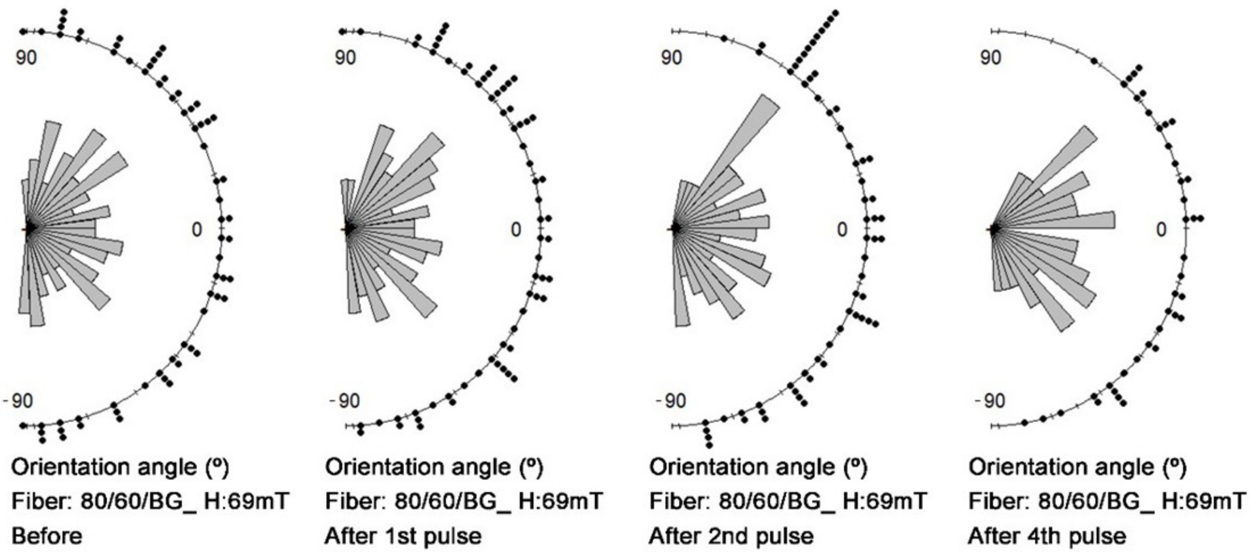

Figure 13. Directional distribution of fibers before and after magnetic alignment through DMP and D-SMP in 2 and 4 pulses of 69 mT at different planar angles of 80/60BG fiber.

At 78 mT the results for fiber 80/60/BG are presented in Figure 14. The charts clearly show a concentration of the fibers in the central area of the sample. From Table 5, the following results can be described in terms of the angular distribution of fibers. The DPM presents a median of 5º, amplitude of 2º and 3º, quartile of 73º and a spread of the sample through $\bar{R}$ of 0.74. D-SMP in two pulses obtained a median of 5º but a reduced angular distribution in quartiles 2 and 3 of 63º and $\bar{R}$ of 0.79. When D-SMP was used in a range of four pulses, the median was 3.5º, the amplitude of quartiles 2-3 of 52.75 and $\bar{R}$ of 0.82.

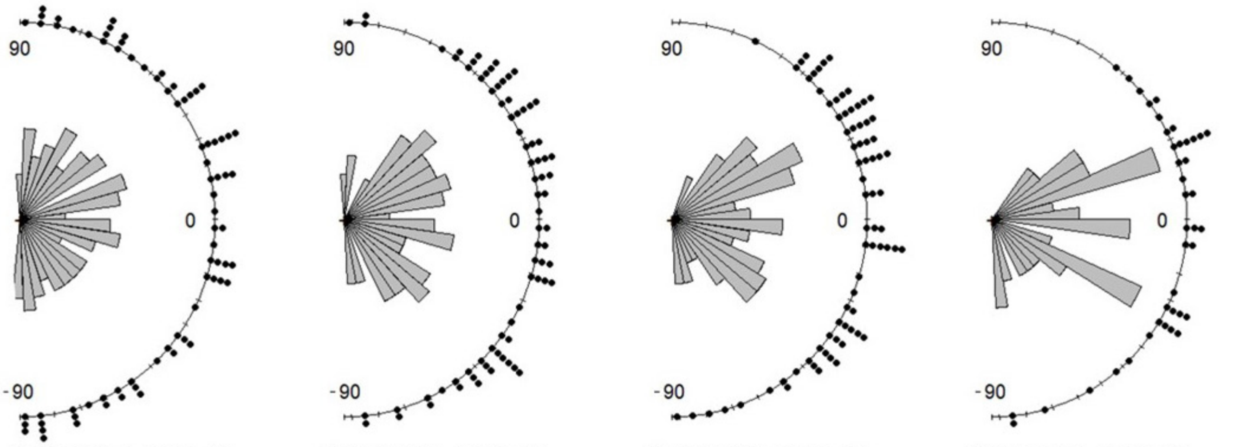

Figure 14. Directional distribution of fibers before and after magnetic alignment through DMP and D-SMP in 2 and 4 pulses of 78 mT at different planar angles of 80/60BG fiber.

3.3. Alignment index

The fiber distribution is described by the alignment index of the samples, as determined by Equation 4. The alignment index defines the main component of the different fibers in the direction considered to be the alignment direction, usually considered by the literature as 0º for well aligned (isotropic) fibers. In Table 3, 4 and 5 the alignment index of HSFs: 45/50, 65/60 and 80/60 respectively can be observed.

The samples with fibers 45/50 presented an alignment index of the samples studied at 30 mT before been exposed to magnetic fields of 0.62 (almost random sample), coming to 0.77 after DMP and increasing again to 0.79 and 0.82 when two or four pulses of D-SMP were applied. The same behavior was observed when 69 mT was applied, showing 0.65 before and 0.87 with DMP and 0.91 after two pulses of D-SMP. More improvement was observed at a higher magnetic field, with an alignment index of 0.94 and 0.96 after DMP and two D-SMP pulses (Table 3).

Batches with 65/60/BG fibers did not show much difference when 30 mT was applied in terms of the alignment index. Slight differences could be found at 69 mT. The alignment index after DMP moved from 0.68 from the initial index to 0.76 and improved to 0.77 and 0.81 when of two and four pulses of D-SMP were applied. When these alignment methods were used at 78 mT, the alignment index increased to 0.84 for DMP and to 0.89 after two D-SMP pulses and to 0.93 after four D-SMP pulses. (Table 4)

The alignment indices for samples with 80/60/BG fibers can be observed in Table 5. Samples under H30 mT maintained values usually observed in randomly orientated samples. However, after being exposed to 68 mT the alignment index increased from 0.61 to 0.67 when the DMP method was used. For two DMPs cycles it improved from 0.61 to 0.69 and to 0.76 for four D-SMP pulses. For samples under a magnetic field of 78 mT, the alignment indices presented values of 0.74 for DMP, 0.79 for two D-SMP pulses and 0.82 for four D-SMP pulses.

3.4. Efficiency factor $\eta\theta_0$

From the results obtained in the directional analysis presented above an efficiency factor ($\eta\theta_0$) according to Krenchel and Cox (30) has been also been obtained to evaluate the improvement according to the increased fiber alignment by both methods. This factor can be considered representative to what can be later expected from the composite as the equation takes in account the amount of fiber in each angle, and not the media as the alignment method.

Table 3. Circular statistics of the study with fiber 45/50/BL.

Fibre Type	Sequence	µ0 H (RMS)	N	sinϑ	cosϑ	$\bar{R}$	Standard Desviation	Initial Angle 1st Quartile	Initial Angle 2nd Quartile	Initial Angle 3rd Quartile (Median)	Initial Angle 4th Quartile	Final Angle 4th Quartile	Alignment Index	Efficiency factor
45/50/BL	Before	30 mT	70	0,1091	0,6227	0,6322	0,9577	-83	-36,50	14,50	55,00	88,00	0,6227	0,3349
45/50/BL	After 1st Pulse	30 mT	70	0,0912	0,7724	0.7778	0.7090	-60	-32,50	12,50	39,75	87,00	0,7724	0,4276
45/50/BL	After 2nd Pulse	30 mT	70	0,0940	0,7913	0.7969	0.6739	-89	-23,25	10,50	33,00	78,00	0,7913	0,4169
45/50/BL	After 4th Pulse	30 mT	50	0,1753	0,821	0.8395	0.5915	-85	-12,25	21,00	33,00	71,00	0,821	0,5169
45/50/BL	Before	69 mT	75	0,0937	0,6498	0.6565	0.9174	-85	-32,50	12,00	50,00	88,00	0,6498	0,3053
45/50/BL	After 1st Pulse	69 mT	75	0,0577	0,8749	0.8768	0.5129	-54	-22,00	11,00	28,50	74,00	0,8749	0,4537
45/50/BL	After 2nd Pulse	69 mT	75	0,0834	0,9179	0.9217	0.4038	-86	-11,00	10,00	20,50	62,00	0,9179	0,4783
45/50/BL	Before	78 mT	75	0,103	0,7064	0.7138	0.8211	-89	-25,00	12,00	41,50	90,00	0,7064	0,3818
45/50/BL	After 1st Pulse	78 mT	75	0,0306	0,9454	0.9459	0.3334	-52	-15,00	11,00	18,00	27,00	0,9454	0,5313
45/50/BL	After 2nd Pulse	78 mT	75	0,0556	0,9622	0.9638	0.2714	-45	-10,00	11,00	15,00	30,00	0,9622	0,5632

Table 4. Circular statistics of the study with fiber 65/60 BG.

Fibre Type	Sequence	µ0 H (RMS)	N	sinϑ	cosϑ	$\bar{\vartheta}\bar{R}$	Standard Desviation	Initial Angle 1st Quartile	Initial Angle 2nd Quartile	Initial Angle 3rd Quartile (Median)	Initial Angle 4th Quartile	Final Angle 4th Quartile	Alignment Index	Efficiency factor
65/60/BG	Before	30	75	0,0579	0,6737	0.6762	0.8846	-88	-35,00	8,00	43,00	90,00	0,6737	0,3506
65/60/BG	After 1st Pulse	30	75	0,0548	0,7024	0.7045	0.8370	-88	-34,00	8,00	41,00	90,00	0,7024	0,368
65/60/BG	After 2nd Pulse	30	75	0,0846	0,6835	0.6887	0.8637	-88	-30,50	4,00	44,50	83,00	0,6835	0,3756
65/60/BG	After 4th Pulse	30	50	0,0621	0,6749	0.6778	0.8819	-87	-30,50	5,00	43,75	82,00	0,6749	0,3868
65/60/BG	Before	69	63	0,1608	0,6818	0.7005	0.8438	-90	-27,50	17,00	49,00	89,00	0,6818	0,4284
65/60/BG	After 1st Pulse	69	63	0,1429	0,7641	0.7774	0.7097	-77	-25,50	15,00	43,50	79,00	0,7641	0,4829
65/60/BG	After 2nd Pulse	69	63	0,1906	0,7745	0.7976	0.6725	-79	-16,00	23,00	39,00	75,00	0,7745	0,4925
65/60/BG	After 4th Pulse	69	38	0,1832	0,818	0.8383	0.5939	-58	-17,75	20,50	38,25	69,00	0,818	0,4961
65/60/BG	Before	78	70	0,1591	0,6665	0.6852	0.8695	-86	-25,00	14,50	51,50	89,00	0,6665	0,3616
65/60/BG	After 1st Pulse	78	70	0,1191	0,8469	0.8552	0.5593	-55	-22,00	14,00	34,50	65,00	0,8469	0,4797
65/60/BG	After 2nd Pulse	78	70	0,1412	0,8884	0.8996	0.4601	-45	-16,00	17,50	29,75	54,00	0,8884	0,5472
65/60/BG	After 4th Pulse	78	50	-0,0494	0,9261	0.9275	0.3881	-52	-25,75	5,50	15,50	31,00	0,9261	0,536

Table 5. Circular statistics of the study with fiber 80/60/BG

Fibre Type	Sequence	µ0 H (RMS)	N	sinϑ	cosϑ	$\bar{\vartheta}\bar{R}$	Standard Desviation	Initial Angle 1st Quartile	Initial Angle 2nd Quartile	Initial Angle 3rd Quartile (Median)	Initial Angle 4th Quartile	Final Angle 4th Quartile	Alignment Index	Efficiency factor
80/60/BG	Before	30	75	0,0783	0,6684	0.6730	0.8900	-82	-35,00	8,00	49,00	90,00	0,6684	0,3039
80/60/BG	After 1st Pulse	30	75	0,0455	0,6894	0.6908	0.8600	-89	-35,50	-2,00	46,00	90,00	0,6894	0,3219
80/60/BG	After 2nd Pulse	30	75	0,1119	0,6494	0.6590	0.9133	-90	-26,00	4,00	57,50	87,00	0,6494	0,3547
80/60/BG	After 4th Pulse	30	50	0,013	0,6517	0.6518	0.9252	-90	-35,50	1,00	48,50	78,00	0,6517	0,3365
80/60/BG	Before	69	65	0,0461	0,6074	0.6094	0.9952	-90	-42,00	3,00	50,00	90,00	0,6074	0,3151
80/60/BG	After 1st Pulse	69	65	0,0437	0,6688	0.6702	0.8946	-85	-41,00	3,00	44,00	89,00	0,6688	0,3478
80/60/BG	After 2nd Pulse	69	65	0,0028	0,6871	0.6871	0.8663	-83	-42,00	2,00	47,00	82,00	0,6871	0,354
80/60/BG	After 4th Pulse	69	40	-0,1134	0,7637	0.7721	0.7192	-82	-40,50	-11,50	30,25	60,00	0,7637	0,394
80/60/BG	Before	78	75	0,0211	0,6247	0.6251	0.9693	-89	-43,00	5,00	43,00	89,00	0,6248	0,3346
80/60/BG	After 1st Pulse	78	75	0,0106	0,7432	0.7432	0.7703	-83	-39,00	5,00	34,00	89,00	0,7432	0,391
80/60/BG	After 2nd Pulse	78	75	-0,0101	0,7918	0.7918	0.6833	-87	-33,50	5,00	29,50	66,00	0,7918	0,4194
80/60/BG	After 4th Pulse	78	40	-0,0613	0,8218	0.8241	0.6220	-83	-29,50	-3,50	23,25	49,00	0,8218	0,4187

Table 3 shows that the values of $\eta\theta_0$ for fiber 45/50 at 30 mT, varying from 0.33 when randomly oriented, to 0.43 after DMP and to 0.41 and 0.52 for two and four D-SMP pulses respectively. This variation is higher for 69 mT as $\eta\theta_0$ is 0.45 for DMP and to 0.48 for two D-SMP pulses. In the case of 78 mT, the results increased up to 0.53 for DMP and up to 0.56 for two D-SMP pulses.

Fiber 65/60/BG do not show a significant variation in $\eta\theta_0$ as the values are similar to before and after the magnetic alignment method when H30 mT is applied. When H is increased to 69 mT the $\eta\theta_0$ moves from 0.43 before aligning, up to 0.48 after the DMP method is applied, and to 0.49 and 0.50 after two and four D-SMP pulses. These values can be seen increased for H79 mT, reaching a $\eta\theta_0$ of 0.48 with the DMP method and 0.55 and 0.54 with D-SMP for two and four pulses respectively.

Table 3 summarizes the results obtained from the study with fiber 80/60/BG. At H30 mT there is a slight variation of $\eta\theta_0$ going from 0.30 before any alignment method is used, to 0.32 after DMP and 0.35 and 0.34 after two and four D-SMP pulses. Increasing H up to 69 mT, the $\eta\theta_0$ does not improve the DMP and two D-SMP pulses maintained a value of 0.35 but improved for four D-SMP up to 0.39. The results obtained for 78 mT presented an improvement of $\eta\theta_0$ reaching values of 0.39 for DMP and of 0.42 for two and four D-SMP pulses.

4. ANALYSIS AND DISCUSSION

The percentage variations (%) of the indices studied in the previous section have been compared for each method and type of fiber. Tables 6-8 present the variation of the indices in comparison to the initial batch before the alignment procedure. The alignment obtained with DMP is lower than that obtained with D-SMP. This can be translated to the final efficiency obtained in the cementitious composites, clearly showing the higher efficiency of D-SMP in two or four pulses compared to DMP.

On the other hand, it should be noted that the efficiency factor in samples is not directly correlated to the alignment index as it takes in account the number of fibers in each section of angles (5º each section). Therefore, this index can be a more precise method to analyze the real effect of the method.

The efficiency factor of each method is not linearly proportional to the magnetic field applied in each case. For instance, it can be observed that for fiber 45/50 the DMP improvement obtained for H30 mT is 24.04%, 34.60% for 69 mT and 33.83% for H78 mT. This variation depends on the initial orientation of the randomly mixed fibers in the composite, but the increase of the magnetic pulse does not lead to a linear increase of the alignment index. In fact, samples with 45/50/BL also present a higher increase in the efficiency factor for H69 mT than for H78 mT. Additionally, for an increase in the magnitude of the magnetic field from 30 to 69 mT (230%) the improvement of $\eta\theta_0$ increases from 27.68% to a 48.61% (Table 6).

A different behavior can be observed in samples with fibers 65/60/BG and 80/60/BG when DMP is applied. First, it must be said that the variation at H30 mT is almost negligible in the alignment index and very low for the efficiency factor. However, the efficiency factor is incremented several times when the magnetic field is increased from 30 to 78 mT. For instance, fiber 65/60/BG increases the alignment index by 4.96% when H is 30 mT, 12.72% when H is 69 mT and 32.66% when H is 78 mT (Table 7).

This means that the increase of the magnetic field should be focused to overcome the T_0^s, and if the fiber rotates, the variation of alignment is not proportional to the magnetic field used. This makes it necessary to study the balance between the fiber and the elastic part of the matrix strain rather than the fiber dynamic in the fluid when the viscosity increase in rate speed is small compared to T_0. This could be also further studied in future research work.

The behavior, mentioned before, can be also observed for fibers under D-SMPs, as the fibers must also exceed T_0^s. Samples with fiber 45/50/BL presented for two pulses in the D-SMP method gave variations of $\eta\theta_0$ of 24.48% for H30 mT, 56.67% for H69 mT and 47.51% for H78 mT. Batches with 80/60BG present a variation of $\eta\theta_0$ of 16.72% for H30 mT, 12.35% for H69 mT and 25.34% for H78 mT. Those batches with fiber 65/60/BG presented increments of $\eta\theta_0$ of 7.13% for H30 mT, 14.96% for H69 mT and 51.33% for H78 mT (Table 8).

As for DMP, the increase of $\eta\theta_0$ is not proportional to H for each fiber studied, being more so for longer fibers (65/60/BG and 80/60/BG). Moreover, it can also be observed that the increase with D-SMP is obtained in cases with low response of the fiber as it is focused on those fibers which can exceed T_0. Therefore, when the window of fibers responding to the magnetic field is wider, the alignment is increased even less proportionally than for DMP. The efficiency increase can be related to an improvement of the homogeneity of the angular distribution of the fibers, as the second and third quartiles are narrower. Moreover, it has been observed after the D-SMP that the angular spread of the fibers is lower.

Table 6. Percentage analysis of the variation of alignment index and efficiency factor in FRCC with fiber 45/50/BL.

Fibre Type	Sequence	μ_0 H (RMS)	% variation alignment index	% variation efficiency factor
45/50/BL	After 1st Pulse	30 mT	24,04%	27,68%
45/50/BL	After 2nd Pulse		27,08%	24,48%
45/50/BL	After 4th Pulse		31,85%	54,34%
45/50/BL	After 1st Pulse	69 mT	34,60%	48,61%
45/50/BL	After 2nd Pulse		41,22%	56,67%
45/50/BL	After 1st Pulse	78 mT	33,83%	39,16%
45/50/BL	After 2nd Pulse		36,21%	47,51%

Table 7. Percentage analysis of the variation of alignment index and efficiency factor in FRCC with fiber 65/60/BG.

Fibre Type	Sequence	μ_0 H (RMS)	% variation alignment index	% variation efficiency factor
65/60/BG	After 1st Pulse	30	4,26%	4,96%
65/60/BG	After 2nd Pulse		1,45%	7,13%
65/60/BG	After 4th Pulse		0,18%	10,33%
65/60/BG	After 1st Pulse	69	12,07%	12,72%
65/60/BG	After 2nd Pulse		13,60%	14,96%
65/60/BG	After 4th Pulse		19,98%	15,80%
65/60/BG	After 1st Pulse	78	27,07%	32,66%
65/60/BG	After 2nd Pulse		33,29%	51,33%
65/60/BG	After 4th Pulse		38,95%	48,23%

Table 8. Percentage analysis of the variation of alignment index and efficiency factor in FRCC with fiber 80/60/BG.

Fibre Type	Sequence	μ_0 H (RMS)	% variation alignment index	% variation efficiency factor
80/60/BG	After 1st Pulse	30	3,14%	5,92%
80/60/BG	After 2nd Pulse		-2,84%	16,72%
80/60/BG	After 4th Pulse		-2,50%	10,73%
80/60/BG	After 1st Pulse	69	10,11%	10,38%
80/60/BG	After 2nd Pulse		13,12%	12,35%
80/60/BG	After 4th Pulse		25,73%	25,04%
80/60/BG	After 1st Pulse	78	18,95%	16,86%
80/60/BG	After 2nd Pulse		26,73%	25,34%
80/60/BG	After 4th Pulse		31,53%	25,13%

It must be also noted that the D-SMP method is not always better when used in four rather than in two pulses. However, this method can result in a future line of work by modifying the angles of the window after each sequence of pulses to be more effective. Moreover, the efficiency factor in some cases does not improve from two D-SMPs to four, as the dynamic of the fiber is low, the rheological torque and the magnetic torque being very similar after the alignment achieved through two pulses. This can be explained as the new angle of the group of fibers presents an angle that reduces the magnetic torque (closer to 0 or well aligned), deriving lower options to rotate. This can be studied by the modification of the sequence of pulses between ($-\Theta_2$, Θ_2) to a new sequence of pulses between ($-\Theta'_2$, Θ'_2).

The results can be compared to other authors who presented an improvement of the alignment index by using a time-maintained, constant magnetic field instead of pulses. Ru Mu (29) presented a combined system of a non-uniform magnetic alignment system and a shake table. The magnetic fields studied applied 0.1/0.2/0.3 T in composites with fibers of length 30 mm and diameter 0.5 mm and hence a shape factor of 60. The efficiency factor increased from 0.5 to a maximum of 0.88 for a magnetic induction intensity of 0.1 T, 0.91 for H0.2 T and 0.93 for H0.3 T. Fibers showed not only an alignment variation but also they were displaced as the magnetic field used was inhomogeneous. The matrix with a viscosity of 1.1 Pa.s also presented some bleeding and segregation when the time was long but no result when the time of exposure to a combined method of shaking plus direct magnetic alignment was short, setting a time of 60 s as recommended (29). In other work, the authors used a circular solenoid that provided an annular magnetic field of 0.05 T to align steel fibers with diameters 0.50 mm and lengths 30 mm in circular-like pipes made of cement-based composite with no or low yield stress and a viscosity 1.1 Pa.s, with alignment indexes from 0.65 to 0.91 (30). We must consider the lower fiber length imparted to the samples studied here and the use of vibration to reduce the static yield stress that facilitated the rotation.

The use of different fibers, not only in their nature but also in their shape factor and length, can be studied in future works. As can be observed from the results, if the factor $\eta\theta_0$ of the three fibers here studied is analyzed, fiber 45/50 presents the best values obtained after the DMP and D-SMP methods are applied to the composites compared to 80/60 and 65/60. The maximum efficiency factor is presented when H was increased as expected to H79 mT composites with fiber 45/50 up to 0.563 with four D-SMP pulses, followed by fiber 65/60 with $\eta\theta_0$ up to 0.5472 after two D-SMP pulses and finally by 80/60 with $\eta\theta_0$ up to 0.4184 after two D-SMP pulses. The improvement of fiber alignment depending on their shape factor also can lead to a more resistant composite with higher toughness, which with the same volume fraction of fibers may increase the amount of fibers in the composite aligned to the maximum stress (8). In the long term, this will also reduce the cracking area and hence the composite will have a longer durability (31, 32). The optimization of fibers through alignment can lead to more cost-effective structures (33), which is one of the problems for using advance cementitious composites such as UHPC (33-34). Moreover, the high-strength steel fibers account nearly a 35% of the total costs of UHPC (35), what can be reduced with a proper alignment method as here shown.

This indicates that the fiber dynamic in the matrix is not linear, and that many factors may influence. From a previous study (17) and from other authors, it that the more flexible the fiber the easier it is to rotate has been analyzed (2). On the other hand, the mass of the fibers in relation to its shape factor (g/mm/mm) is also important to achieve a higher magnetic torque and hence rotate (Table 1). If we compare this relationship from fibers 65/60 to fibers 80/60, it passes from 4.8 to 2.75 g/mm/mm, and therefore the magnetic torque can be double comparing both fibers; and although the first one is less flexible, the second one presents a lower magnetic torque. This is in line with the results obtained, as fiber 80/60 presents a lower efficiency factor and a lower response to rotate. The same difference can be observed when fiber 45/50 and 65/60 are compared (7.40g/mm/mm and 4.80 g/mm/mm respectively), although the first one shows higher rigidity it also has higher mass and then higher magnetic moment than the 65/60 fiber.

Initial rotation must exceed the static yield stress, and after this happens and during rotation, the shear stress reduces the speed of the fiber. The time for final alignment must last for at least the time to achieve the rotation during which the magnetic torque is also reduced, as the sine of theta is lower and lower until final alignment (sine of 0º=0). This will be also a factor to consider the angle to the first misalignment pulse to reinforce the torque in the second alignment pulse.

Although the final alignment angle in the one pulse and the two pulses processes are slightly improved with the two pulse process in some cases, an improvement of the homogeneity of the angular distribution of the fibers can be clearly observed. The deviation is lower, and hence the angular variation between fibers and the efficiency is higher.

D-SMP presented a higher efficiency factor that can allow this method to be applied in composites presenting a higher T_0^s at the moment of manufacture, caused by the rheological properties of the fluid or their change in time. As can be observed in the literature, the method could be further studied with other fibers coated with ferromagnetic layer. J.Xu et al. studied composites with carbon fibers of $7.5 \cdot 10^{-3}$ mm coated with a layer made of nickel with a thickness of $0.25 \cdot 10^{-3}$ mm, and a viscosity of fresh cement paste employed ranging from 1.0 Pa·s to 10.0 Pa·s, increasing the alignment factor from 0.532 to 0.909 in composites with a 0.2 wt (%) fibers, to 0.874 when the wt (%) of fibers increased to 0.3, and to 0.801 in composites with 0.3 wt (%) of carbon fibers (36). L.Liu et J.Xu studied composites with nickel-coated Carbon Nano-Tubes (CNTs) as reinforcement. CNTs were 30–50 nm in diameter and 10–20 µm in length with an orientation factor of value of about 0.75 for cement-based composites (37).

The use of two perpendicular pairs of coils (two Helmholtz coils) can allow the setting of different angles for homogeneous magnetic fields by using different magnetic fields in every pulse simultaneously, setting the angle Θ_2 for the D-SMP method. This can be also studied in industrial samples with higher dimensions.

5. CONCLUSIONS

The alignment method through directional-sequenced magnetic pulses increases the effectiveness of the magnetic field. In this work a matrix with T_0, Carpopol™ has been used as a metaphor fluid for cementitious composites, to determine the angular response of the fibers. This novel method increases the fiber alignment index and the efficiency factor of the composite, thanks to an enhanced angular homogeneity of the reinforcement with denser alignment along the desired alignment direction.

To set the required parameters of the angular direction of the directional-sequenced magnetic pulses a study of the fiber response and angles between the fiber rotation has been performed. The magnetic field and the matrix rheological properties can be studied through statistical analysis to set the angles between the magnetic pulses and the composite.

Moreover, it has been observed that in the magnetic field alignment processes, the mass of the fiber in relation to its shape factor must be high to achieve a high magnetic torque but it needs enough flexibility to increase its ability to rotate. Hence fiber design must be considered as part of the alignment method since both its geometry and properties determine its magnetic and rheological moment. Additionally, factors that determine the magnetizing field such as the coil design, time of pulse, direction of the pulse and rheological properties of the matrix require careful consideration.

Acknowledgement

This research was funded by the Spanish Science Ministry, Grant number PID2020-119707RB-I00 (Orientación de fibras de refuerzo en hormigón para edificación mediante campos magnéticos). The support from the Universidad de las Palmas de Canaria, and especially the help of the Building Construction and Structures Laboratory of Escuela de Arquitectura de Las Palmas de Gran Canaria, are also highly acknowledged.

Authorship contribution statement

Nelson Flores Medina: Conceptualization, Funding acquisition, Investigation, Methodology, Project administration, Resources, Validation, Visualization, Writing – original draft.

Laura Trigo Ramírez: Data curation, Formal analysis, Investigation, Writing – review & editing.

Víctor Pérez Villar: Conceptualization, Formal analysis, Supervision, Validation, Visualization, Writing – review & editing.

Víctor Cabrera García: Data curation, Formal analysis, Investigation.

Francisco Gil Carrillo: Formal analysis, Validation, Visualization.

Declaration of competing interest

The authors of this article declare that they have no financial, professional or personal conflicts of interest that could have inappropriately influenced this work.

REFERENCES

1. Yoo DY, Banthia N. 2016. Mechanical properties of ultra-high-performance fiber-reinforced concrete: A review. Cem. Concr. Compos. 73:267-280. https://doi.org/10.1016/j.cemconcomp.2016.08.001
2. Martinie L, Rossi P, Roussel N. 2010. Rheology of fiber reinforced cementitious materials: classification and prediction. Cem. Concr. Res. 40(2):226–234. https://doi.org/10.1016/j.cemconres.2009.08.032
3. Martinie L, Roussel N. 2011. Simple tools for fiber orientation prediction in industrial practice. Cem. Concr. Res. 41(10):993–1000. https://doi.org/10.1016/j.cemconres.2011.05.008
4. Li L, Wei YJ, Li Z, Farooqi MU. 2022. Rheological and viscoelastic characterizations of fly ash/slag/silica fume-based geopolymer. J. Clean. Prod. 354:131629. https://doi.org/10.1016/j.jclepro.2022.131629
5. Hajforoush M, Kheyroddin A, Rezaifar O. 2020. Investigation of engineering properties of steel fiber reinforced concrete exposed to homogeneous magnetic field. Constr. Build. Mater. 252:119064. https://doi.org/10.1016/j.conbuildmat.2020.119064
6. Abavisani I, Rezaifar O, Kheyroddin A. 2018. Alternating magnetic field effect on fine-aggregate steel chip–reinforced concrete properties. J. Mater. Civ. Eng. 30(6):04018097. https://doi.org/10.1061/(ASCE)MT.1943-5533.0002267
7. Javahershenas F, Sohrabi Gilani M, Hajforoush M. 2021. Effect of magnetic field exposure time on mechanical and microstructure properties of steel fiber-reinforced concrete (SFRC). J. Build. Eng. 35:101975. https://doi.org/10.1016/j.jobe.2020.101975
8. da Silva Brito I, Strauss Rambo DA, Martini S, Salvador RP, de Menezes Freitas MF. 2021. Flexural behavior of HPFRCC: Enhancing post-crack strength and toughness by magnetic alignment of the reinforcement. Constr. Build. Mater. 269:121265. https://doi.org/10.1016/j.conbuildmat.2020.121265
9. Wijffels MJH, Wolfs RJM, Suiker ASJ, Salet TAM. 2017. Magnetic orientation of steel fibres in self-compacting concrete beams: Effect on failure behaviour. Cem. Concr. Compos. 80:342-355. https://doi.org/10.1016/j.cemconcomp.2017.04.005

10. Wang X, Xu B, Mu R, Qing L, Liu Y, Chen X, Chen J, Lei Z. 2023. Flexural properties of a 2D-distributed steel fiber reinforced cement-based composite two-way slab. J. Build. Eng. 73:106792. https://doi.org/10.1016/j.jobe.2023.106792
11. Cao G, Li Z, Jiang S, Tan Y, Li Z, Long S, Tong Z. 2022. Experimental analysis and numerical simulation of flow behavior of fresh steel fibre reinforced concrete in magnetic field. Constr. Build. Mater. 347:128505. https://doi.org/10.1016/j.conbuildmat.2022.128505
12. Carrera K, Künzel K, Konrad P, Mara M, Kheml P, Papež V, Savjak R. 2023. The effect of magnetic field parameters on fibre orientation in high-performance fibre-reinforced concrete. Mech. Mater. 177:104534. https://doi.org/10.1016/j.mechmat.2022.104534
13. Coussot P. 2005. Rheometry of Pastes suspensions and granular materials: Applications in Industry. New York: J Wiley & Sons. https://doi.org/10.1002/0471720577
14. Pérez Villar V, Flores Medina N. 2018. Alignment of hooked-end fibres in matrices with similar rheological behaviour to cementitious composites through homogeneous magnetic fields. Constr. Build. Mater. 163:256–266. https://doi.org/10.1016/j.conbuildmat.2017.12.084
15. Kheml P, Carrera K, Künzel K, Papež V, Sovják R. 2022. Summary of findings on magnetic orientation of fibers in cement composites. Mater. Today Proc. 58:1104–1107. https://doi.org/10.1016/j.matpr.2022.01.201
16. Mu R, Diao C, Liu H, Wu H, Qing L, Zhao S, Li L. 2021. Design, preparation and mechanical properties of full-field aligned steel fiber reinforced cementitious composite. Constr. Build. Mater. 272:121631. https://doi.org/10.1016/j.conbuildmat.2020.121631
17. Pérez Villar V, Flores Medina N, Alonso MM, Gismera Diez S, Puertas F. 2019. Assessment of parameters governing the steel fiber alignment in fresh cement-based composites. Constr. Build. Mater. 207:548–562. https://doi.org/10.1016/j.conbuildmat.2019.02.036
18. Chen J, Wang J, Jin WL. 2016. Study of magnetically driven concrete. Constr. Build. Mater. 121:53–59. https://doi.org/10.1016/j.conbuildmat.2016.05.152
19. Jaworski Z, Spychaj T, Story A, Story G. 2021. Carbomer microgels as model yield-stress fluids. Rev. Chem. Eng. 38(7):881-919. https://doi.org/10.1515/revce-2020-0016
20. Hernández MJ, Pellicer J, Delegido J, Dolz M. 1998. Rheological characterization of easy-to-disperse (etd) carbopol hydrogels. J. Dispersion Sci. Technol. 19(1):31–42. https://doi.org/10.1080/01932699808913159
21. Shyshko S, Mechtcherine V. 2013. Developing a Discrete Element Model for simulating fresh concrete: Experimental investigation and modelling of interactions between discrete aggregate particles with fine mortar between them. Constr. Build. Mater. 47:601–615. https://doi.org/10.1016/j.conbuildmat.2013.05.071
22. Spangenberg J, Roussel N, Hattel JH, Stang H, Skocek J, Geiker MR. 2012. Flow induced particle migration in fresh concrete: Theoretical frame, numerical simulations and experimental results on model fluids. Cem. Concr. Res. 42(4):633-641. https://doi.org/10.1016/j.cemconres.2012.01.007
23. Kelessidis V, Hatzistamou V. 2011. Preparation Methodology and Rheological Properties of Yield Pseudoplastic Transparent Fluids. J. Dispersion Sci. Technol. 32(3):380-388. https://doi.org/10.1080/01932691003662399
24. Künzel K, Papež V, Carrera K, Konrád P, Mára M, Kheml P, Sovják R. 2021. Electromagnetic properties of steel fibres for use in cementitious composites, fibre detection and non-destructive testing. Materials. 14(9):2131. https://doi.org/10.3390/ma14092131
25. Fisher NI. 1993. Statistical analysis of circular data. Cambridge: Cambridge University Press. https://doi.org/10.1017/CBO9780511564345
26. Pérez Villar V, Flores Medina N, Trigo Ramírez L. 2024. Correlation through directional statistics of the consequences of magnetic alignment of steel fibers immersed in metaphor fluids of cementitious matrices. Constr. Build. Mater. 444:137714. https://doi.org/10.1016/j.conbuildmat.2024.137714
27. Krenchel H. 1975. Fibre spacing and specific fibre surface. In: RILEM Symposium on Fibre Reinforced Cement and Concrete. Pags. 69–79.
28. Harris B. 1999. Engineering composite materials. New York: Taylor and Francis.
29. Mu R, Dong R, Liu H, Chen H, Cheng Q, Fan C. 2021. Preparation of aligned steel-fiber-reinforced concrete using a magnetic field created by the assembly of magnetic pieces. Crystals. 11(7):837. https://doi.org/10.3390/cryst11070837
30. Mu R, Xue Y, Qing L, Li H, Zhao Y, Zhou J, Su J. 2019. Preparation and mechanical performance of annularly aligned steel fiber reinforced cement-based composite pipes. Constr. Build. Mater. 211:167–173. https://doi.org/10.1016/j.conbuildmat.2019.03.146
31. Du J, Meng W, Khayat KH, Bao Y, Guo P, Lyu Z, Abu-obeidah A, Nassif H, Wang H. 2021. New development of ultra-high-performance concrete (UHPC). Compos. Part B Eng. 224:109220. https://doi.org/10.1016/j.compositesb.2021.109220
32. Banthia N, Sappakittipakorn M. 2007. Toughness enhancement in steel fiber reinforced concrete through fiber hybridization. Cem. Concr. Res. 37:1366–1372. https://doi.org/10.1016/j.cemconres.2007.05.005
33. Meng W, Valipour M, Khayat K. 2017. Optimization and performance of cost-effective ultra-high performance concrete. Mater. Struct. 50:29. https://doi.org/10.1617/s11527-016-0896-3
34. Wille K, Kim DJ, Naaman AE. 2011. Strain-hardening UHP-FRC with low fiber contents. Mater. Struct. 44:583–598. https://doi.org/10.1617/s11527-010-9650-4
35. Yoo DY, Kim S, Park GJ, Park JJ, Kim SW. 2017. Effects of fiber shape, aspect ratio, and volume fraction on flexural behavior of ultra-high-performance fiber-reinforced cement composites. Compos. Struct. 174:375–388. https://doi.org/10.1016/j.compstruct.2017.04.069
36. Xu J, Yin T, Wang Y, Liu L. 2021. Anisotropic electrical and piezoresistive sensing properties of cement-based sensors with aligned carbon fibers. Cem. Concr. Compos. 116:103873. https://doi.org/10.1016/j.cemconcomp.2020.103873
37. Liu L, Xu J, Yin T, Wang Y, Chu H. 2021. Improved conductivity and piezoresistive properties of Ni-CNTs cement-based composites under magnetic field. Cem. Concr. Compos. 121:104089. https://doi.org/10.1016/j.cemconcomp.2021.104089